

See discussions, stats, and author profiles for this publication at: <https://www.researchgate.net/publication/7444997>

Kinetics of the Oxidation of Phenols and Phenolic Endocrine Disruptors during Water Treatment with Ferrate (Fe(VI))

ARTICLE *in* ENVIRONMENTAL SCIENCE AND TECHNOLOGY · DECEMBER 2005

Impact Factor: 5.33 · DOI: 10.1021/es051198w · Source: PubMed

CITATIONS

101

READS

125

3 AUTHORS, INCLUDING:



Yunho Lee

Gwangju Institute of Science and Technology

34 PUBLICATIONS 1,169 CITATIONS

SEE PROFILE

Kinetics of the Oxidation of Phenols and Phenolic Endocrine Disruptors during Water Treatment with Ferrate (Fe(VI))

YUNHO LEE,^{†,‡} JEYONG YOON,^{*,†} AND URS VON GUNTEN^{*,‡}

School of Chemical and Biological Engineering,
College of Engineering, Seoul National University, San 56-1,
Sillim-dong, Gwanak-gu, 151-742 Seoul, Korea, and
Swiss Federal Institute for Aquatic Science and Technology,
EAWAG, 8600 Dübendorf, Switzerland

The ability of ferrate (Fe(VI)) to oxidize phenolic endocrine-disrupting chemicals (EDCs) and phenols during water treatment was examined by determining the apparent second-order rate constants (k_{app}) for the reaction of Fe(VI) with selected environmentally relevant phenolic EDCs (17 α -ethinylestradiol, β -estradiol, and bisphenol A) and 10 substituted phenols at pH values ranging from 6 to 11. The three selected groups of EDCs showed appreciable reactivity with Fe(VI) (k_{app} at pH 7 ranged from 6.4×10^2 to $7.7 \times 10^2 \text{ M}^{-1} \text{ s}^{-1}$). The k_{app} for the substituted phenols studied at pH 7 ranged from 6.6 to $3.6 \times 10^3 \text{ M}^{-1} \text{ s}^{-1}$, indicating that many other potential phenolic EDCs can be oxidized by Fe(VI) during water treatment. The Hammett-type correlations were determined for the reaction between HFeO_4^- and the undissociated ($\log(k) = 2.24\text{--}2.27\sigma^+$) and dissociated phenol ($\log(k) = 4.33\text{--}3.60\sigma^+$). A comparison of the Hammett correlation obtained for the reaction between HFeO_4^- and dissociated phenol with those obtained from other drinking water oxidants revealed that HFeO_4^- is a relatively mild oxidant of phenolic compounds. The effectiveness of Fe(VI) for the oxidative removal of phenolic EDCs was also confirmed in both natural water and wastewater.

Introduction

In recent years, there has been increasing concern about the widespread occurrence of endocrine-disrupting chemicals (EDCs), pharmaceuticals, and personal care products (PPCPs) in the aquatic environment (1). EDCs are released into aquatic environments as a result of industrial, agricultural, and sewage runoff. EDCs, such as steroid estrogens and alkylphenols, have been found in sewage or wastewater treatment effluents at concentrations in the nanogram per liter to microgram per liter range (2), indicating that they are only partially removed via existing treatment processes. As a result, EDCs (i.e., steroid estrogens) have been sometimes found in surface waters at concentrations sufficient to cause changes in the endocrine functions of wildlife (20–200 pg L^{-1} range) (3).

* Address correspondence to either author. Phone: +82-02-880-8927 (J.Y.); +41-1-823-5270 (U.v.G.). Fax: +82-02-876-8911 (J.Y.); +41-1-823-5028 (U.v.G.). E-mail: jeyong@snu.ac.kr (J.Y.); vungunten@eawag.ch (U.v.G.).

[†] Seoul National University.

[‡] Swiss Federal Institute for Aquatic Science and Technology.

Recent studies have shown that several oxidants, such as ozone, chlorine dioxide, and chlorine, can be applied to control many EDCs in drinking water and wastewater treatment (4–6). In particular, ozonation is highly effective in treating EDCs with a phenolic moiety. Huber et al. reported that ozonation could rapidly oxidize the phenolic moiety of 17 α -ethinylestradiol (EE2) (second-order rate constant of $\sim 3 \times 10^6 \text{ M}^{-1} \text{ s}^{-1}$ at pH 7), resulting in a rapid decrease in the estrogenic activity (7).

Ferrate (Fe(VI)) is an emerging water treatment chemical that can be used as both an oxidant and a coagulation agent (8, 9). As a single oxidant, Fe(VI) oxidizes reduced sulfur- and nitrogen-containing compounds (e.g., hydrogen sulfide and hydrazine), phenols, amines, and alcohols (8, 9). As a result of its combined oxidant and coagulant effects, Fe(VI) has been demonstrated to be quite effective in removing arsenic and copper(I) cyanide from water (10, 11). Despite the high potential of Fe(VI) as a new water treatment chemical, information on the reactivity of Fe(VI) toward various organic functional groups under the conditions relevant to water treatment is limited. Although several rate constants for the reaction between Fe(VI) and reactive moieties have been reported, they were usually obtained under basic pH conditions (pH > 8) because of experimental restrictions due to the instability of ferrate at lower pH (8, 9). In addition, the pH dependency of the rate constants has not been clearly explained in some cases using the known pH-dependent speciation of Fe(VI) and organic functional groups. For example, Rush et al. (12) reported a second-order rate constant for the reaction between phenol and Fe(VI) as $100 \text{ M}^{-1} \text{ s}^{-1}$ at pH values ranging from 5.5 to 10. A constant rate is unexpected because both Fe(VI) and phenol have a species distribution within the pH range studied (the pK_a 's for $\text{HFeO}_4^-/\text{FeO}_4^{2-}$ and PhOH/PhO^- are 7.23 and 9.99, respectively), and the reactivity of each species of Fe(VI) and phenol is quite different (8, 9, 13).

Fe(VI) has been known to react via one-electron or two-electron transfer depending on its reaction counterparts (9). As an example of one-electron transfer, the oxidation of phenol by Fe(VI) was proposed to produce phenoxyl radicals and Fe(V) through a hydrogen abstraction mechanism (12, 14). A two-electron transfer mechanism was suggested for the oxidation of sulfite by Fe(VI) through a direct oxygen transfer mechanism, generating sulfate and Fe(IV) (15). Fe(V) and Fe(IV) are known to be several orders of magnitude more reactive than Fe(VI) (16). Therefore, oxidation rates of pollutants by Fe(VI) may be enhanced when reactions are conducted in the presence of one-electron or two-electron reducing substrates.

The phenolic moiety is a substructure of many important classes of EDCs such as steroid estrogens and alkylphenols and is responsible for their biological effects. Therefore, kinetic information on the reaction between Fe(VI) and various substituted phenols can be quite useful in assessing the potential of Fe(VI) for oxidizing phenolic EDCs during water treatment. Recently, two studies reported that Fe(VI) could effectively remove some phenolic EDCs (bisphenol A, estrone, and 17 β -estradiol) in both a synthetic buffer solution and in real wastewater (17, 18). However, in these studies the rate constants for this reaction were not determined, yielding only case-specific information on the removal efficiency.

The aim of the present study was to determine the potential of Fe(VI) for the oxidative removal of phenolic EDCs and various phenols during water treatment in the pH range of 6–11. This was possible because of a new analytical method

with a high sensitivity for the measurement of Fe(VI) (19). To assess the potential for EDC oxidation, the second-order rate constants for the reaction of Fe(VI) with selected phenolic EDCs, 17 α -ethinylestradiol (EE2), 17 β -estradiol (E2), and bisphenol A (BPA) were measured (see Figure S1 in the Supporting Information). These EDCs were chosen because of their environmental relevance (2, 3). The second-order rate constants for the reaction between Fe(VI) and various substituted phenols were also measured to predict the rate constants for reactions with additional phenolic water contaminants including phenolic EDCs. In addition, the measured rate constants for the substituted phenols were compared with the rate constants available for other drinking water oxidants. Finally, oxidation experiments of the selected phenolic EDCs were performed in both natural water and wastewater.

Experimental Section

Standards and Reagents. High-purity (>95%) potassium ferrate (K₂FeO₄) was prepared using the method of Thompson et al. (20). Stock solutions of Fe(VI) (100–300 μ M) were prepared by dissolving solid samples of K₂FeO₄ in a 5 mM Na₂HPO₄/1 mM borate buffer (pH \approx 9.1), where aqueous Fe(VI) is known to be most stable (8, 9). 17 α -ethinylestradiol, β -estradiol, bisphenol A, and several substituted phenols were purchased from Sigma-Aldrich and were of the highest purity available. Stock solutions of phenolic EDCs (10 μ M) were first prepared in 0.1 M NaOH solution and then neutralized by using concentrated HClO₄. Ultrapurified water (> 18 M Ω cm) was obtained using a Barnstead B-Pure system.

Analytical Methods. EE2, E2, and BPA were determined using high-performance liquid chromatography (HPLC, Hewlett-Packard, 1050 series) with a fluorescence detector (HP 1064A) (see text S2 in the Supporting Information). The Fe(VI) concentrations were determined using the ABTS method at 415 nm (19). The pH measurements were carried out using a Metrohm 632 pH meter (Metrohm, Herisau, Switzerland), which was calibrated using standard buffers (pH 4, 7, and 9, Merck). The spectrophotometric measurements were performed on a Uvikon 940 spectrophotometer (Kontron Instrument, Eching, Germany).

Determination of Rate Constants. On the basis of preliminary experiments, the reaction order between Fe(VI) and all the phenolic compounds investigated in this study was found to be first order with respect to Fe(VI) and the phenolic compounds (see text S3 in the Supporting Information). Therefore, the apparent second-order rate constants could be determined using pseudo-first-order kinetic conditions with either Fe(VI) or the phenolic compounds in excess (see text S4 in the Supporting Information). All the kinetic experiments were performed in a batch reactor at 25 $^{\circ}$ C. The rate constants were measured in the pH range of 6–11. At each pH, the rate measurements were performed once or twice and the values were averaged. The reaction solutions were buffered using a 25 mM phosphate buffer in the pH range of 6–8 and 25 mM phosphate/5 mM borate in the pH range of 9–12. A phosphate buffer was used throughout the pH range investigated because phosphate prevents Fe(III) precipitation (8, 9), which might interfere with the accurate determinations of the rate constants. pH changes during the experiments were $\leq \pm 0.1$ units.

Oxidation in Natural Water and Wastewater. Treatment of phenolic EDCs by Fe(VI) under realistic conditions was simulated with experiments in natural water and wastewater. Natural water was taken from Lake Zürich, Switzerland (DOC = 1.6 mg L⁻¹, alkalinity = 2.5 mM as HCO₃⁻, and pH = 7.9) (Lake Zürich water). For the wastewater, the secondary effluent of a conventional activated sludge treatment (CAS) at a municipal wastewater treatment plant in Kloten-Opfikon, Switzerland (DOC = 5.3 mg L⁻¹, alkalinity = 3.5 mM as HCO₃⁻,

and pH = 7.8) was used (Kloten wastewater) (see text S5 in the Supporting Information). As a first step, single-dosage experiments were carried out to assess the competition for Fe(VI) between the water matrix and the phenolic EDCs (EE2, E2, and BPA). The Lake Zürich water or Kloten wastewater was buffered to pH 8 with a borate buffer (10 mM). The water was then spiked with one phenolic EDC (0.15 μ M) and transferred into six 25 mL serum vials. Then, Fe(VI) doses of 0.10, 0.25, 0.5, 1.0, and 2.0 mg L⁻¹ were injected into the vials while the water was vigorously stirred for a few seconds. After 30 min, the reaction solution was treated with 0.5 mL of ascorbic acid (25 mM) to quench the reaction. The sample was then immediately acidified to pH below 2.5 with 0.5 mL of concentrated HClO₄ to minimize precipitation of Fe(III). Sample analysis was carried out without sample filtration within a few hours using the HPLC methods described above. The experiments were performed in duplicate. As a second step, kinetic experiments to test whether the rate constants obtained in pure water can be applied to predict the oxidation kinetics of phenolic EDCs in real water were performed in Lake Zürich water and Kloten wastewater spiked with EE2 or BPA and then treated with Fe(VI). A 250 mL glass bottle with a dispenser system mounted onto the screwtop was used as a reaction vessel. The kinetic runs were started by addition of Fe(VI). The samples (5 mL) for the analysis of phenolic EDCs were withdrawn using the dispenser system at appropriate time intervals and immediately quenched with ascorbic acid and acidified with HClO₄. The Fe(VI) concentrations were measured simultaneously in a second sample by the ABTS method (19). All experiments in natural water and wastewater were performed at 25 $^{\circ}$ C.

Results and Discussion

Kinetics for the Reactions of EE2, E2, and BPA with Fe(VI).

The reactions of Fe(VI) and the phenolic EDCs are first order with respect to each reactant and can be described by eq 1.

$$-d[\text{EDC}]_{\text{tot}}/dt = k_{\text{app}}[\text{Fe(VI)}]_{\text{tot}}[\text{EDC}]_{\text{tot}} \quad (1)$$

where k_{app} represents the apparent second-order rate constant for the reaction of Fe(VI) with each EDC (EE2, E2, and BPA) as a function of pH, $[\text{Fe(VI)}]_{\text{tot}}$ represents the total concentration of Fe(VI) species, and $[\text{EDC}]_{\text{tot}}$ represents the total concentration of each EDC species.

Figure 1 shows that k_{app} of the three phenolic EDCs exhibited a similar pH dependency, which generally decreased with increasing pH. These pH dependencies of k_{app} can be attributed to a combination of effects derived from Fe(VI) speciation and phenolic EDCs speciation. Fe(VI) is a diprotic acid ($\text{H}_2\text{FeO}_4 = \text{HFeO}_4^- + \text{H}^+$, $\text{p}K_{\text{a,H}_2\text{FeO}_4} = 3.50$ (21) and $\text{HFeO}_4^- = \text{FeO}_4^{2-} + \text{H}^+$, $\text{p}K_{\text{a,HFeO}_4^-} = 7.23$ (22)). The three phenolic EDCs are monoprotic acids (EE2 and E2) or diprotic acid (BPA) for their phenolic moieties (See Table 1 for their $\text{p}K_{\text{a}}$ values). The pH dependency of k_{app} for each phenolic EDC could be quantitatively modeled by eq 2.

$$k_{\text{app}}[\text{Fe(VI)}]_{\text{tot}}[\text{EDC}]_{\text{tot}} = \sum_{\substack{i=1,2,3 \\ j=1,2,3}} k_{ij}\alpha_i\beta_j[\text{Fe(VI)}]_{\text{tot}}[\text{EDC}]_{\text{tot}} \quad (2)$$

where $[\text{Fe(VI)}]_{\text{tot}} = [\text{H}_2\text{FeO}_4] + [\text{HFeO}_4^-] + [\text{FeO}_4^{2-}]$, $[\text{EDC}]_{\text{tot}} = [\text{EDC}] + [\text{EDC}^-] + [\text{EDC}^{2-}]$, α_i and β_j represent the respective species distribution coefficients for Fe(VI) and phenolic EDC, i and j represents each of the three Fe(VI) species and phenolic EDC species, respectively, and k_{ij} represents the species-specific second-order rate constant for the reaction between the Fe(VI) species i with the phenolic EDC species j .

The reactions of H_2FeO_4 and FeO_4^{2-} with the phenolic EDCs did not appear to contribute significantly to the overall

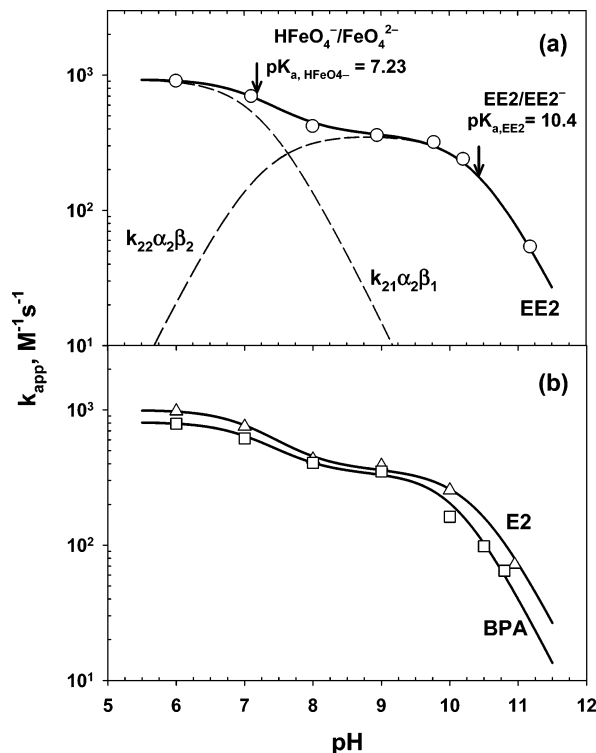
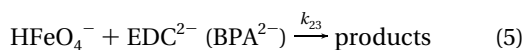
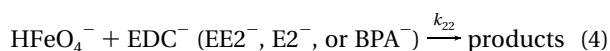
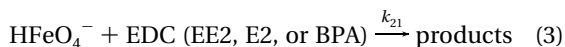


FIGURE 1. pH dependency of the apparent second-order rate constants for the reactions between Fe(VI) and the selected phenolic EDCs (pH range of 6–11 and 25 °C): (a) 17α-ethinyloestradiol (EE2) and (b) β-estradiol (E2) and bisphenol A (BPA). The symbols represent the measured data, and the lines represent the model calculations. The dashed lines in (a) represent the contribution of the reaction between HFeO_4^- and EE2 ($k_{21}\alpha_2\beta_1$) and EE2 ($k_{22}\alpha_2\beta_2$) to the overall reaction as a function of pH.

reaction and thus were neglected in the model calculations (see text S6 in the Supporting Information). Therefore, the following reactions (eqs 3–5) can be considered as main reactions between Fe(VI) and the phenolic EDCs to explain the pH dependency of the reaction rates.



When considering the above reactions, the apparent second-order rate constant, k_{app} , is given by eq 6 or 7 (see text S7 in the Supporting Information):

$$k_{app} = k_{21}\alpha_2\beta_1 + k_{22}\alpha_2\beta_2 \quad \text{for EE2 and E2} \quad (6)$$

$$k_{app} = k_{21}\alpha_2\beta_1 + k_{22}\alpha_2\beta_2 + k_{23}\alpha_2\beta_3 \quad \text{for BPA} \quad (7)$$

The species-specific second-order rate constants, k_{ij} , were calculated using least-squares regression of the experimental k_{app} data (see text S8 in the Supporting Information). A good correlation between the experimental and modeled values was obtained, as shown in Figure 1. Table 1 summarizes the determined moiety-specific rate constants. As expected from their molecular structure, the three phenolic EDCs showed similar rate constants. The rate constants for the reaction between HFeO_4^- and the undissociated phenolic EDCs (k_{21}) were calculated to be $(0.8\text{--}1.0) \times 10^3 \text{ M}^{-1} \text{s}^{-1}$, and the rate constants for the reaction between HFeO_4^- and the dissoci-

TABLE 1. Specific Second-order Rate Constants for the Reactions of Fe(VI) with Selected Phenolic EDCs and Substituted Phenols in the pH Range of 6–11 and at 25 °C (the Errors in Parentheses Refer to One Standard Deviation)

no.	compounds	pK_a	σ^{+a}	σ^b	$k_{12} (\text{M}^{-1} \text{s}^{-1})$	$k_{21} (\text{M}^{-1} \text{s}^{-1})$	$k_{22} (\text{M}^{-1} \text{s}^{-1})$	$k_{23} (\text{M}^{-1} \text{s}^{-1})$	$k_{app} \text{ at pH 7} (\text{M}^{-1} \text{s}^{-1})$
1	17α-ethinyloestradiol (EE2)	10.4 ^b	c	c	$9.4 (\pm 0.2) \times 10^2$	$5.4 (\pm 0.2) \times 10^5$	7.3×10^2		
2	β-estradiol (E2)	10.4 ^b	c	c	$1.0 (\pm 0.02) \times 10^3$	$5.4 (\pm 0.2) \times 10^5$	7.7×10^2		
3	bisphenol A (BPA)	9.6/10.2 ^d	c	c	$8.2 (\pm 0.1) \times 10^2$	$8.0 (\pm 0.2) \times 10^4$	6.4×10^2	$2.6 (\pm 0.2) \times 10^5$	
4	2,4-dimethylphenol	10.58 ^e	-0.62	-0.34	$5.0 (\pm 0.3) \times 10^3$	$2.5 (\pm 0.4) \times 10^6$	3.6×10^3		
5	4-methylphenol	10.26 ^e	-0.31	-0.17	$9.6 (\pm 0.2) \times 10^2$	$2.4 (\pm 0.2) \times 10^5$	6.9×10^2		
6	4-(tert)-butylphenol	10.23 ^e	-0.26	-0.20	$5.8 (\pm 0.3) \times 10^2$	$1.4 (\pm 0.2) \times 10^5$	4.2×10^2		
7	phenol	9.99 ^e	0	0	$1.0 (\pm 0.04) \times 10^2$	$2.1 (\pm 0.2) \times 10^4$	7.7×10^1		
8	4-chlorophenol	9.43 ^e	0.11	0.23	$1.5 (\pm 0.1) \times 10^2$	$1.8 (\pm 0.1) \times 10^4$	1.3×10^2		
9	4-bromophenol	9.34 ^e	0.15	0.23	$8.0 (\pm 0.4) \times 10^1$	$1.2 (\pm 0.04) \times 10^4$	8.6×10^1		
10	4-carboxylatophenol	9.23 ^e	0.42	0.45	$2.0 (\pm 0.02) \times 10^1$	$1.0 (\pm 0.02) \times 10^3$	1.6×10^1		
11	4-sulfonatophenol	8.80 ^f	c	0.35	$6.5 (\pm 0.4) \times 10^0$	$2.7 (\pm 0.2) \times 10^2$	6.6×10^0		
12	4-cyanophenol	7.86 ^g	0.66	0.66	$2.2 (\pm 0.05) \times 10^6$	$7.0 (\pm 0.4) \times 10^1$	5.8×10^1		
13	4-nitrophenol	7.15 ^h	0.79	0.78	$3.7 (\pm 0.1) \times 10^5$	$1.5 (\pm 0.2) \times 10^1$	3.4×10^1		

^a Calculated from ref 27. ^b From ref 23. ^c Not available in the literature (see text S9 in the Supporting Information for the estimated σ^+ values of EE2, E2, and BPA). ^d From ref 24. ^e From ref 25. ^f From ref 13. ^g From ref 26.

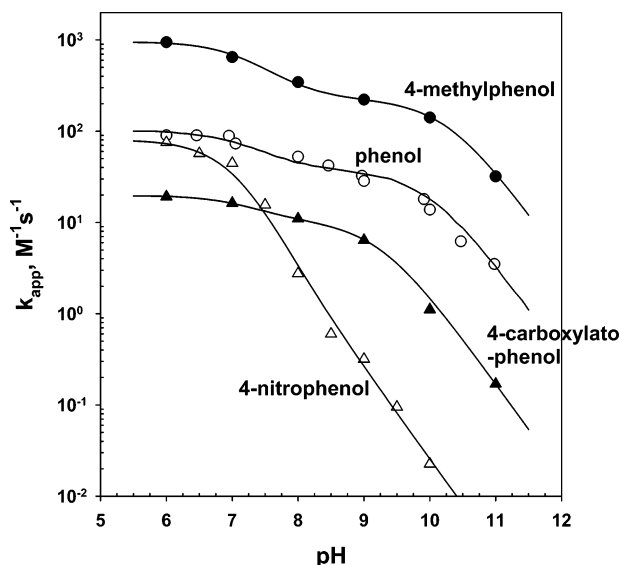


FIGURE 2. pH dependency of the apparent second-order rate constants for the reactions between Fe(VI) and the selected substituted phenols (pH range of 6–11 and 25 °C). The symbols represent the measured data, and the lines represent the model calculations. The lines for 4-methylphenol, phenol, and 4-carboxylatophenol were obtained using eq 6. The line for 4-nitrophenol was obtained using eq 9.

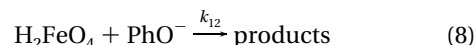
ated phenolic EDCs (k_{22} and k_{23}) were calculated to be $(0.8\text{--}5.4) \times 10^5 \text{ M}^{-1} \text{ s}^{-1}$. Hence, the k_{22} or k_{23} was $\sim(1\text{--}6) \times 10^2$ fold higher than k_{21} . These differences can be explained by the higher activating effect of the hydroxyl groups as a result of their deprotonation. For EE2, the reaction between HFeO_4^- and the dissociated EE2 ($k_{22}\alpha_2\beta_2$) controls the overall reaction at $\text{pH} \geq 7.5$, and the reaction between HFeO_4^- with the undissociated EE2 ($k_{21}\alpha_2\beta_1$) dominates at $\text{pH} < 7.5$, as shown in Figure 1a (dash lines). This trend was also found for E2 and BPA (data not shown).

Kinetics for the Reactions of Substituted Phenols with Fe(VI). To determine the general reactivity of Fe(VI) with phenols, the apparent second-order rate constants (k_{app}) of the Fe(VI) reaction with 10 different substituted phenols were measured at pH values ranging from 6 to 11. Figure 2 shows the k_{app} of selected substituted phenols as a function of pH. The k_{app} generally decreased with increasing pH for all the substituted phenols. The observed pH dependency can be explained by the kinetic model used for interpreting the kinetic data of EE2 and E2 (eq 6).

For all the substituted phenols studied except for 4-cyanophenol and 4-nitrophenol, eq 6 can successfully explain the observed pH dependency of the k_{app} , as shown in Figure 2. To distinguish each pH profile, only the k_{app} data and prediction results of 4-methylphenol, phenol, and 4-carboxylatophenol are shown. The specific second-order rate constants, k_{21} and k_{22} , were calculated using least-squares regression analysis, and Table 1 summarizes the values obtained for the corresponding phenols (denoted as nos. 4–11).

For 4-cyanophenol and 4-nitrophenol, eq 6 fails to explain the observed pH dependency of k_{app} . For 4-nitrophenol, the k_{app} steadily increases even at $\text{pH} < 7.5$ (open triangle in Figure 2) where the HFeO_4^- concentration is at its maximum ($\text{pK}_{\text{a,HFeO}_4^-} = 7.23$) and the abundance of dissociated phenols are decreasing steeply ($\text{pK}_{\text{a,4-nitrophenol}} = 7.15$) (Table 1). In addition, Figure 2 shows that the k_{app} value of 4-nitrophenol ($75.4 \text{ M}^{-1} \text{ s}^{-1}$) at pH 6 was much higher than that of 4-carboxylatophenol ($19.2 \text{ M}^{-1} \text{ s}^{-1}$). This was not expected because the nitro substituent is known to have a stronger deactivating effect on the oxidation rate of the substituted

phenols than the carboxylato substituent (13). A similar unexpected pH dependency of k_{app} was observed for 4-cyanophenol (data not shown). To explain the pH dependency of k_{app} of 4-cyanophenol and 4-nitrophenol, the following reaction between H_2FeO_4 species and the dissociated phenol species ($k_{12}\alpha_1\beta_2$) was considered along with the reactions of HFeO_4^- .



The significant contribution of reaction 8 to the overall reaction can be expected for 4-cyanophenol and 4-nitrophenol for the following three reasons. First, the fraction of the dissociated forms (β_2) of 4-cyanophenol and 4-nitrophenol is higher than that of the other phenols within the studied pH range examined (6–11) because their pK_{a} values are significantly lower than those of the other phenols (see Table 1). In addition, the highest rate for the reaction of H_2FeO_4 with the dissociated forms ($\alpha_1\beta_2$) of 4-cyanophenol and 4-nitrophenol is expected at $\text{pH } 5.4\text{--}5.7$ ($\text{pH}_{\text{max}} = (\text{pK}_{\text{a,H}_2\text{FeO}_4} + \text{pK}_{\text{a,phenol}})/2$). This can explain the steady increase in k_{app} at $\text{pH} < 7.5$. Last, H_2FeO_4 is known to have a higher reactivity than HFeO_4^- ($k_{12} \gg k_{22}$) (28). Therefore, it can significantly contribute to the overall reaction even though its concentration is very low (less than 10^{-8} M). Under the above assumption, the k_{app} is given by eq 9 (see text S7 in the Supporting Information):

$$k_{\text{app}} = (k_{12}\alpha_1\beta_2 + k_{21}\alpha_2\beta_1 + k_{22}\alpha_2\beta_2) \quad (9)$$

Least-squares regression analysis using eq 9 shows a successful model for the observed pH dependency of k_{app} for 4-cyanophenol and 4-nitrophenol as shown in Figure 2. The k_{12} values determined were 2.2×10^6 and $3.7 \times 10^5 \text{ M}^{-1} \text{ s}^{-1}$ for 4-cyanophenol and 4-nitrophenol, respectively. These rate constants are $\sim(2\text{--}3) \times 10^4$ times higher than k_{22} , which were determined to be 7.0×10^1 and $1.5 \times 10^1 \text{ M}^{-1} \text{ s}^{-1}$ for 4-cyanophenol and 4-nitrophenol, respectively. The k_{22} for 4-cyanophenol and 4-nitrophenol are consistent with the decreasing trend of k_{22} for the phenols with more electron-withdrawing substituents as shown in Table 1. The values of k_{21} could not be determined accurately, suggesting that the contribution of $k_{21}\alpha_2\beta_1$ is relatively low compared with those of $k_{12}\alpha_1\beta_2$ and $k_{22}\alpha_2\beta_2$.

Linear Free Energy Relationships. The Hammett substituent constants (σ^+ , σ , and σ^-) were used to predict the effect of the substituents on the rate constants of the substituted phenols (27). For the values of k_{21} and k_{22} (Table 1, nos. 4–13), the Hammett-type correlations were tested using three sets of σ constants (σ^+ , σ , and σ^-). The best Hammett-type correlations were obtained when using σ^+ (see text S9 in the Supporting Information). Figure 3 shows the obtained Hammett-type correlations for k_{21} versus σ^+ (Table 1, nos. 4–10) and for k_{22} versus σ^+ (Table 1, nos. 4–13 except for no. 11). The linear regressions for both the undissociated and the dissociated phenols are

$$\log(k_{21}) = 2.24 (\pm 0.05) - 2.27 (\pm 0.17)\sigma^+ \\ r^2 = 0.974, n = 7 \quad (10)$$

$$\log(k_{22}) = 4.33 (\pm 0.08) - 3.60 (\pm 0.18)\sigma^+ \\ r^2 = 0.983, n = 9 \quad (11)$$

A negative Hammett slope (ρ) is expected for electrophilic oxidation. The magnitude of the ρ value reflects the sensitivity of the reaction to the substituent effect (27). Therefore, the reaction between HFeO_4^- with the dissociated phenols ($\rho = -3.60$) is more sensitive to the substituent effect than that with the undissociated phenols ($\rho = -2.27$).

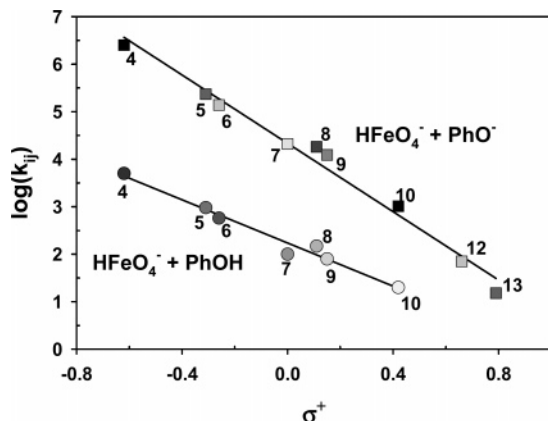


FIGURE 3. Correlations between the second-order rate constants of the reactions between HFeO_4^- with the undissociated phenols (k_{21}) and the dissociated phenols (k_{22}) vs Hammett σ^+ constants. The numbers of the compounds correspond to those in Table 1.

Correlation analysis for k_{21} and k_{22} with pK_a values of substituted phenols are also tested. The pK_a value reflects the effect of the substituents on the electron density of the aromatic ring. In addition, the correlation based on the pK_a values can be more practical in predicting the rate constants for the oxidation of phenolic compounds by Fe(VI) because pK_a values are more readily accessible than the σ^+ constants. Good linear relationships for both k_{21} (Table 1, nos. 4–11) and k_{22} (Table 1, nos. 4–13) are found with the pK_a values. In addition, the obtained linear relationships predict successfully the rate constants for the reaction of Fe(VI) with EE2, E2, and BPA (see Figure S5 in the Supporting Information). This indicates the usefulness of the obtained linear relationships to predict rate constants for the reaction of Fe(VI) with phenolic compounds of complex structure.

Because Fe(VI) is a relatively new oxidant, a comparison between the reactivity of Fe(VI) toward phenolic compounds with those of other drinking water oxidants is needed. For this, the Hammett-type correlation for the reaction between HFeO_4^- and the dissociated phenols (k_{22}) versus σ was compared with those of other oxidants, such as ozone (O_3) (29), chlorine dioxide (ClO_2) (13), hypiodous acid (HOI) (26), hypobromous acid (HOBr) (30), and hypochlorous acid (HOCl) (31). Hammett-type correlations based on σ rather than σ^+ were compared since σ has been usually used to obtain Hammett-type correlations for most other drinking water oxidants. Hammett-type correlations for the reaction between the oxidants and undissociated phenols could not be compared because the correlations were found to be very poor for the other oxidants. The obtained correlation equation for k_{22} versus σ (Table 1, nos. 4–13) is

$$\log(k_{22}) = 4.66 (\pm 0.16) - 4.30 (\pm 0.38)\sigma$$

$$r^2 = 0.940, n = 10 \quad (12)$$

Figure 4 shows that the k_{22} of HFeO_4^- are several orders of magnitude lower than those of O_3 , HOBr, ClO_2 , and HOI but are comparable to that of HOCl. Therefore, HFeO_4^- seems to be a relative mild oxidant for the oxidation of phenolic compounds compared with other drinking water oxidants except for HOCl. The Hammett slope for HFeO_4^- ($\rho = -4.3$) was higher than the values found for O_3 ($\rho = -2.1$), HOBr ($\rho = -3.3$), ClO_2 ($\rho = -3.4$), and HOCl ($\rho = -3.0$) but lower than the value obtained for HOI ($\rho = -7.1$). This indicates that HFeO_4^- is more sensitive to substitution effects than the other drinking water oxidants with the exception of HOI.

Oxidative Removal of EDCs in Natural Water and Wastewater. Experiments for the removal of EE2, E2, and BPA were performed in real waters to apply the rate constants

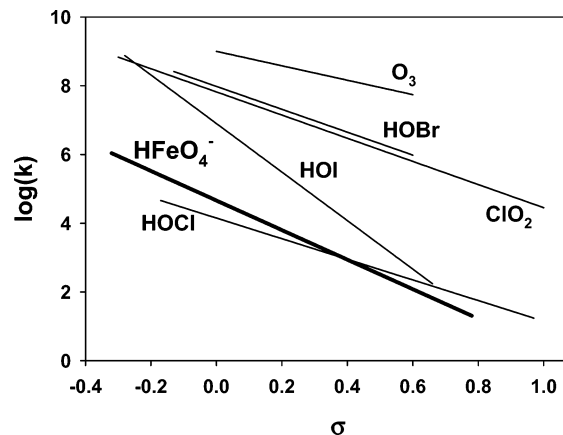


FIGURE 4. Comparison of the correlations between the second-order rate constants of the reaction (k_{22}) between the dissociated phenols and HFeO_4^- , O_3 , ClO_2 , HOI, HOBr, and HOCl vs the Hammett σ constants. The correlation for O_3 , ClO_2 , HOI, HOBr, and HOCl were taken from refs 29, 13, 26, 30, and 31, respectively.

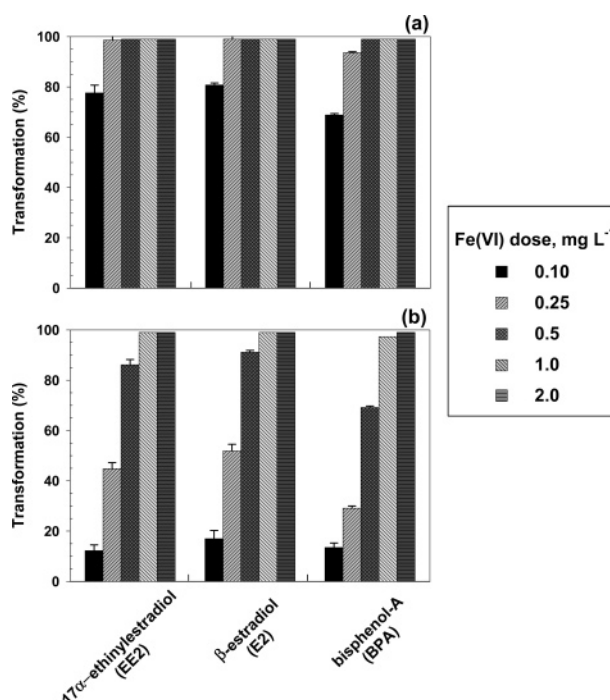


FIGURE 5. Oxidation of EE2, E2, and BPA (a) in natural water (Lake Zürich water, $\text{DOC} = 1.6 \text{ mg L}^{-1}$) and (b) wastewater (Kloten wastewater, $\text{DOC} = 5.3 \text{ mg L}^{-1}$) as a function of the Fe(VI) dose (0.1–2.0 mg L^{-1}). Experimental conditions: $\text{pH} = 8$, $T = 25^\circ\text{C}$, $[\text{EDCs}]_0 = 0.15 \mu\text{M}$, and contact time = 30 min. Transformations up to 99% could be measured using the existing detection limits.

determined in this study to realistic treatment conditions. The determined second-order rate constants of EE2, E2, and BPA oxidation by Fe(VI) at near neutral pH (6–8) ranged from 400 to 900 $\text{M}^{-1} \text{s}^{-1}$, indicating that these phenolic EDCs can be significantly removed during water treatment with Fe(VI) at a dose of a few milligrams per liter within 30 min. However, when Fe(VI) is applied to real water, which has a substantial Fe(VI) demand, the phenolic EDCs and the water matrix will compete for Fe(VI). Therefore, the phenolic EDCs may not be completely transformed below a certain Fe(VI) dose. Figure 5 shows the oxidation of EDCs in Lake Zürich water and Kloten wastewater at various Fe(VI) doses between 0.1 and 2.0 mg L^{-1} and a contact time of 30 min. For Lake Zürich water, a dose of 0.5 mg L^{-1} was sufficient to remove 99% of the initial concentrations (0.15 μM) of EE2, E2, and

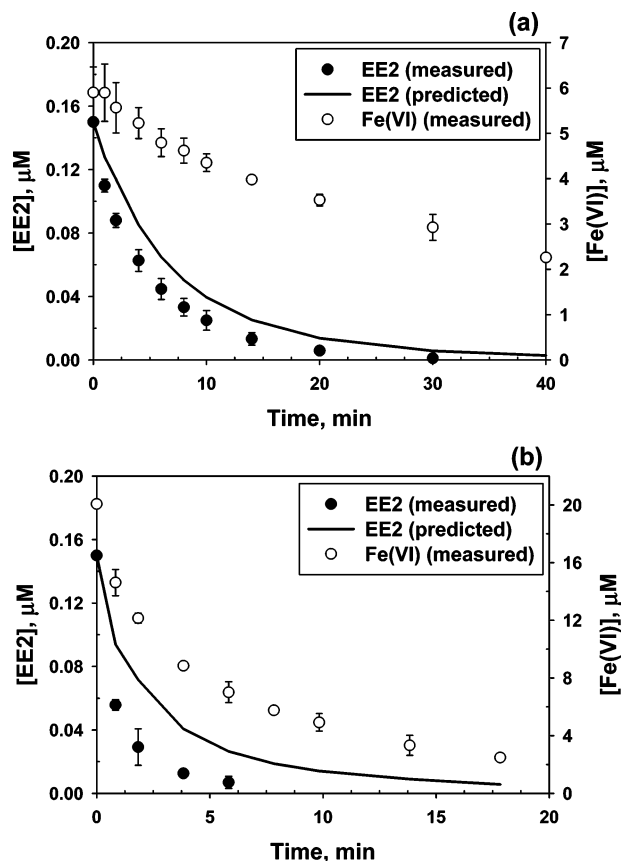


FIGURE 6. Oxidation kinetics of EE2 by Fe(VI) during the treatment of (a) lake water and (b) wastewater. The symbols represent the measured data, and the solid lines represent the model predictions. Experimental conditions: pH = 8 and $T = 25\text{ }^{\circ}\text{C}$.

BPA (Figure 5a). For Kloten wastewater, a dose of more than 1 mg L^{-1} was needed to achieve 99% removal (Figure 5b). The lower removal efficiency for Kloten wastewater can be explained by the higher DOM (dissolved organic matter) concentration of the Kloten wastewater (5.3 mg L^{-1} as C) than that of Lake Zürich water (1.6 mg L^{-1} as C), resulting in a higher Fe(VI) demand. Overall, these results demonstrate that relatively low Fe(VI) doses (a few milligrams per liter) are sufficient to achieve a significant transformation of EE2, E2, and BPA in both a natural water and a wastewater containing high concentration of natural organic matter.

To investigate the dynamics of EDC oxidation, both Lake Zürich water and Kloten wastewater were spiked with $0.15\text{ }\mu\text{M}$ EE2 and BPA and treated with Fe(VI) at a dose of 6 and $20\text{ }\mu\text{M}$, respectively. These experiments were carried out to test if the rate constants estimated for pure water could be used to predict the oxidation kinetics of low levels of phenolic EDCs in real waters (nanograms per liter range). The following equation can be used to predict the extent of oxidation of a target compound (E), when $[E] \ll [\text{Fe(VI)}]$:

$$\frac{[E]_t}{[E]_0} = \exp[-k_{\text{Fe(VI)}} \int_0^t [\text{Fe(VI)}] dt] \quad (13)$$

where $k_{\text{Fe(VI)}}$ is the second-order rate constant for the reaction with Fe(VI) and $\int_0^t [\text{Fe(VI)}] dt$ is the Fe(VI) exposure (Fe(VI) concentration integrated over time) within a contact time of t .

According to eq 13, predictions can be made if $k_{\text{Fe(VI)}}$ and the corresponding Fe(VI) exposure are known. Figure 6 shows the time-dependent EE2 and Fe(VI) concentrations (circles) during the treatment of the Lake Zürich water (Figure 6a)

and Kloten wastewater (Figure 6b), respectively. The predictions in Figure 6 show that the determined rate constants ($k_{\text{Fe(VI)}} = 4.5 \times 10^2\text{ M}^{-1}\text{ s}^{-1}$ at pH 8) can be used to predict the EE2 oxidation kinetics in real water reasonably well (lines). A comparable prediction was also found in the case of BPA (see text S10 in the Supporting Information).

Nevertheless, the prediction slightly underestimated the level of EE2 and BPA removal in the both waters. One explanation for this is the contribution of Fe(V) or Fe(IV) species to the oxidation of EE2 and BPA. In the model buffer solution where the rate constants were measured, the decay of Fe(VI) occurs mainly by its self-decomposition. During the self-decomposition, Fe(VI) first form a dimeric intermediate of Fe(VI). The dimeric intermediate oxidizes water producing oxygen and ferric ion, which might not involve a significant generation of Fe(V) or Fe(IV) species (21). In contrast, in real water Fe(VI) decays mainly via a reaction with natural organic matter, which might generate significant concentrations of Fe(V) or Fe(IV) species (9). However, additional experiments will be needed to clarify their roles in the oxidation process using Fe(VI) because detailed kinetic information on the Fe(V)/Fe(IV) reactions are not available in the literature.

Acknowledgments

This work was supported by Grant R01-2003-000-10053-0 from the Basic Research Program of the Korea Science and Engineering Foundation. Financial support from the Brain Korea 21 project is also acknowledged. The authors would like to thank Elisabeth Salhi for her laboratory support.

Supporting Information Available

Text and figures addressing (1) structures of selected phenolic EDCs; (2) HPLC measurements of phenolic EDCs; (3) order of reaction between Fe(VI) and phenol; (4) determination of the second-order rate constant; (5) description of real waters; (6) contribution of each Fe(VI) and phenolic EDC species to the overall reaction; (7) ionization fraction of Fe(VI) and phenolic compounds; (8) least-squares regression analysis; (9) linear free energy relationships; (10) oxidation kinetics in natural water and wastewater. This material is available free of charge via the Internet at <http://pubs.acs.org>.

Literature Cited

- Kolpin, D. W.; Furlong, E. T.; Meyer, M. T.; Thurman, E. M.; Zaugg, S. D.; Barber, L. B.; Buxton, H. T. Pharmaceuticals, hormones, and other organic wastewater contaminants in U. S. streams, 1999–2000: A national reconnaissance. *Environ. Sci. Technol.* **2002**, *36*, 1202–1211.
- Esperanza, M.; Suidan, M. T.; Nishimura, F.; Wang, Z.-M.; Sorial, G. Z.; Zaffiro, A.; Mccauley, P.; Brenner, R.; Sayles, G. Determination of sex hormones and nonylphenol ethoxylates in the aqueous matrixes of two pilot-scale municipal wastewater treatment plants. *Environ. Sci. Technol.* **2004**, *38*, 3028–3035.
- Kuch, H. M.; Ballschmiter, K. Determination of endocrine-disrupting phenolic compounds and estrogens in surface and drinking water by HRGC-(NCI)-MS in the pictogram per liter range. *Environ. Sci. Technol.* **2001**, *35*, 3201–3206.
- Huber, M. M.; Canonica, S.; Park, G.-Y.; von Gunten, U. Oxidation of pharmaceuticals during ozonation and advanced oxidation processes. *Environ. Sci. Technol.* **2003**, *37*, 1016–1024.
- Huber, M. M.; Korhonen, S.; Ternes, T. A.; von Gunten, U. Oxidation of pharmaceuticals during water treatment with chlorine dioxide. *Water Res.* **2005**, *39*, 3607–3617.
- Deborde, M.; Rabouan, S.; Gallard, H.; Legube, B. Aqueous chlorination kinetics of some endocrine disruptors. *Environ. Sci. Technol.* **2004**, *38*, 5577–5583.
- Huber, M. M.; Ternes, T. A.; von Gunten, U. Removal of estrogenic activity and formation of oxidation products during ozonation of 17α -ethinylestradiol. *Environ. Sci. Technol.* **2004**, *38*, 5177–5186.
- Sharma, V. K. Potassium ferrate(VI). An environmentally friendly oxidant. *Adv. Environ. Res.* **2002**, *6*, 143–156.

- (9) Lee, Y.; Cho, M.; Kim, J.; Yoon, J. Chemistry of ferrate (Fe(VI)) in aqueous solution and its applications as a green chemical. *J. Ind. Eng. Chem.* **2004**, *10*, 161–171.
- (10) Lee, Y.; Um, I.-H.; Yoon, J. Arsenic(III) oxidation by iron(III) (ferrate) and subsequent removal of arsenic(V) by iron(III) coagulation. *Environ. Sci. Technol.* **2003**, *37*, 5750–5756.
- (11) Sharma, V. K.; Burnett, C. R.; Yngard R. A.; Cabelli, D. E. Iron(VI) and iron(V) oxidation of copper(I) cyanide. *Environ. Sci. Technol.* **2005**, *39*, 3849–3854.
- (12) Rush, J. D.; Cyr, J. E.; Zhao, Z.; Bielski, B. H. J. The oxidation of phenol by ferrate(VI) and ferrate(V). A pulse radiolysis and stopped-flow study. *Free Radical Res.* **1995**, *22*, 349–360.
- (13) Tratnyek, P. G.; Hoigné, J. Kinetics of reactions of chlorine dioxide (OCIO) in water-II. Quantitative structure–activity relationship for phenolic compounds. *Water Res.* **1994**, *28*, 57–66.
- (14) Huang, H.; Sommerfeld, D.; Dunn, B. C.; Eyring, E. M.; Lloyd, C. R. Ferrate(VI) oxidation of aqueous phenol: Kinetics and Mechanism. *J. Phys. Chem. A* **2001**, *105*, 3536–3541.
- (15) Goff, H.; Murmann, R. K. Studies on the mechanism of isotopic oxygen exchange and reduction of ferrate(VI) ion (FeO_4^{2-}). *J. Am. Chem. Soc.* **1971**, *93*, 6058–6065.
- (16) Sharma, V. K.; O'Connor, D. B.; Cabelli, D. E. Sequential one-electron reduction of Fe(V) to Fe(III) by cyanide in alkaline medium. *J. Phys. Chem. B* **2001**, *105*, 11529–11532.
- (17) Jiang, J. Q.; Yin, Q.; Zhou, J. L.; Pearce, P. Occurrence and treatment trials of endocrine disrupting chemicals (EDCs) in wastewaters. *Chemosphere*, **2005**, *61*, 544–550.
- (18) Li, C.; Li, X. Z.; Graham, N. A study of the preparation and reactivity of potassium ferrate. *Chemosphere*, **2005**, *61*, 537–543.
- (19) Lee, Y.; Yoon, J.; von Gunten, U. Spectrophotometric determination of ferrate (Fe(VI)) in water by ABTS. *Water Res.* **2005**, *39*, 1946–1953.
- (20) Thompson, G. W.; Ockerman, L. T.; Schreyer, J. M. Preparation and purification of potassium ferrate. *J. Am. Chem. Soc.* **1951**, *73*, 1379–1381.
- (21) Rush, J. D.; Zhao, Z.; Bielski, B. H. J. Reaction of ferrate(VI)/ferrate(V) with hydrogen peroxide and superoxide anion—a stopped-flow and premix pulse radiolysis study. *Free Radical Res.* **1996**, *24*, 187–198.
- (22) Sharma, V. K.; Burnett, C. R.; Millero, F. J. Dissociation constants of the monoprotic ferrate(VI) ion in NaCl media. *Phys. Chem. Chem. Phys.* **2001**, *3*, 2059–2062.
- (23) Clarke, E. G.; Moffat, A. C. In *Clark's Isolation and Identification of Drugs*; The Pharmaceutical Press: London, 1986.
- (24) Kosky, P. E.; Guggenheim, E. A. The aqueous phase in the interfacial synthesis of polycarbonates. 1. Ionic equilibria and experimental solubilities in the BAP–NaOH–H₂O system. *Ind. Eng. Chem. Res.* **1991**, *30*, 462–467.
- (25) Dean, J. A. *Lange's Handbook of Chemistry*; McGraw-Hill: New York, 1992.
- (26) Bichsel, Y.; von Gunten, U. Formation of iodo-trihalomethanes during disinfection and oxidation of iodide-containing waters. *Environ. Sci. Technol.* **2000**, *34*, 2784–2791.
- (27) Hansch, C.; Leo, A.; Taft, R. W. A survey of Hammett substituent constants and resonance and field parameters. *Chem. Rev.* **1991**, *91*, 165–195.
- (28) Kamachi, T.; Kouno, T.; Yoshizawa, K. Participation of multi-oxidants in the pH dependence of the reactivity of ferrate(VI). *J. Org. Chem.* **2005**, *70*, 4380–4388.
- (29) Hoigné, J.; Bader, H. Rate constants of reactions of ozone with organic and inorganic compounds in water-II. *Water Res.* **1983**, *17*, 185–194.
- (30) Gallard, H.; Pellizzari, F.; Philippe, J.; Legube, C. B. Rate constants of reactions of bromine with phenols in aqueous solution. *Water Res.* **2003**, *37*, 2883–2892.
- (31) Gallard, H.; von Gunten, U. Chlorination of phenols: Kinetics and formation of chloroform. *Environ. Sci. Technol.* **2002**, *36*, 884–890.

Received for review June 24, 2005. Revised manuscript received September 14, 2005. Accepted September 15, 2005.

ES051198W

Supporting Information for
Kinetics of the Oxidation of Phenols and Phenolic Endocrine Disruptors
during Water Treatment with Ferrate (Fe(VI))

Yunho Lee^{1,2}, Jeyong Yoon^{*1}, and Urs von Gunten^{**2}

¹*School of Chemical and Biological Engineering, College of Engineering, Seoul National
University, San 56-1, Sillim-dong, Gwanak-gu, 151-742 Seoul, Korea*

²*Swiss Federal Institute for Aquatic Science and Technology, EAWAG, 8600 Dübendorf,
Switzerland*

Submitted to
Environmental Science & Technology

^{*1}Corresponding author, e-mail: jeyong@snu.ac.kr, phone: +82-02-880-8927; fax: +82-02-876-8911

^{**2}Co-corresponding author, e-mail: vongunten@eawag.ch, phone: +41-1-823-5270; fax: +41-1-823-5028

This document was prepared on 13th, September, 2005, as a Supporting Information of ES05 1198w, consisted of 14 pages including 10 texts and 6 figures.

Text S1. Structures of Selected Phenolic EDCs.

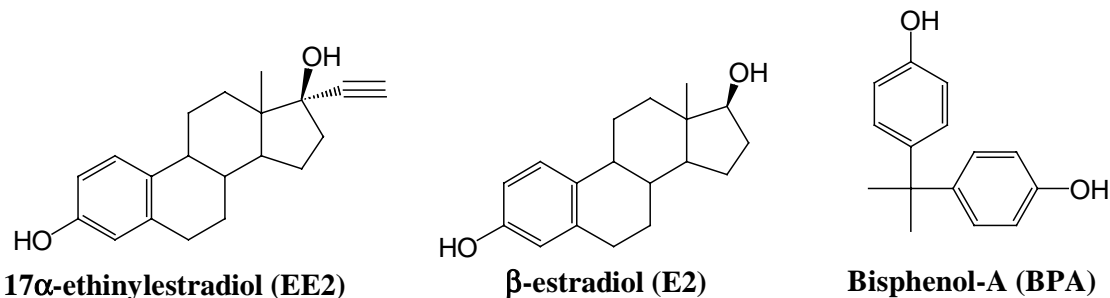


Figure S1. Structures of the selected phenolic EDCs, 17 α -ethinylestradiol (EE2), 17 β -estradiol (E2), and bisphenol-A (BPA).

Text S2. Phenolic EDCs Determination by HPLC Method.

EE2, E2, and BPA were determined using high-performance liquid chromatography (HPLC, Hewlett-Packard, 1050 series) with a fluorescence detector (HP 1064A). A C-18 reverse phase column (Nucleosil 100, 5- μ m, Machery-Nagel) was used as the stationary phase with 0.6 mL min⁻¹ of the eluent consisting of 50% acetonitrile and 50% 10 mM phosphoric acid. An excitation wavelength of 229 nm and an emission wavelength of 309 nm were used to detect the fluorescence. The detection limits were ~ 5 nM for all three phenolic EDCs (EE2, E2, and BPA) for an injection volume of 100 μ L. The 95% confidence interval for a single measurement was typically $\pm 5\%$.

Text S3. Order of Reaction between Fe(VI) and Phenol.

The general rate expression for the reaction between Fe(VI) and phenol (PhOH) can be written as

$$-d[\text{Fe(VI)}]_{\text{T}}/dt = k_{\text{app}}[\text{Fe(VI)}]_{\text{tot}}^a [\text{PhOH}]_{\text{tot}}^b \quad (1)$$

where $[\text{Fe(VI)}]_{\text{tot}}$ and $[\text{PhOH}]_{\text{tot}}$ are the molar concentrations of the total Fe(VI) ($\text{H}_n\text{FeO}_4^{n-2}$) and PhOH species (PhOH/PhO^-), respectively; a and b are the orders of the reaction; k_{app} is the apparent rate constant of the reaction between Fe(VI) and PhOH.

The kinetic experiments were undertaken under pseudo-first-order conditions for Fe(VI), where an excess of PhOH was used ($[\text{Fe(VI)}]_{\text{tot}} < 2 \mu\text{M}$ and $[\text{PhOH}]_{\text{tot}} > 50 \mu\text{M}$). Under these conditions, eq 1 can be rewritten as

$$-d[\text{Fe(VI)}]_{\text{tot}}/dt = k' [\text{Fe(VI)}]_{\text{tot}}^a \quad (2)$$

where $k' = k_{\text{app}} [\text{PhOH}]_{\text{tot}}^b$

The pseudo-first-order rate constants for the decrease of Fe(VI) (k') were obtained by measuring the decrease of Fe(VI) concentration as a function of time in the presence of excess PhOH. Figure S2, as representative data at $[\text{PhOH}]_{\text{tot}} = 500 \mu\text{M}$ and $\text{pH} = 9.0$ (25 mM phosphate/5 mM borate buffer), shows that Fe(VI) follows a pseudo-first order decrease ($R^2 > 0.99$) with a rate constant of $1.6 \times 10^{-2} \text{ s}^{-1}$, confirming that the reaction is first-order with respect to Fe(VI) ($a = 1$). Then, k' values were determined at various concentrations of PhOH (50–500 μM) at $\text{pH} = 9.0$. In all cases, the decrease of Fe(VI) was confirmed to be first-order with respect to Fe(VI) ($R^2 > 0.99$). Figure S3 clearly shows the linearity of k' with respect to $[\text{PhOH}]_{\text{tot}}$ ($R^2 > 0.99$), confirming this reaction to also be first-order with respect to PhOH ($b = 1$). From the slope in Fig. S3, the apparent second-order rate constant for the reaction between Fe(VI) and PhOH, $k_{\text{app}} = 3.2 \times 10^1 \text{ M}^{-1} \text{ s}^{-1}$ was obtained at $\text{pH} 9.0$.

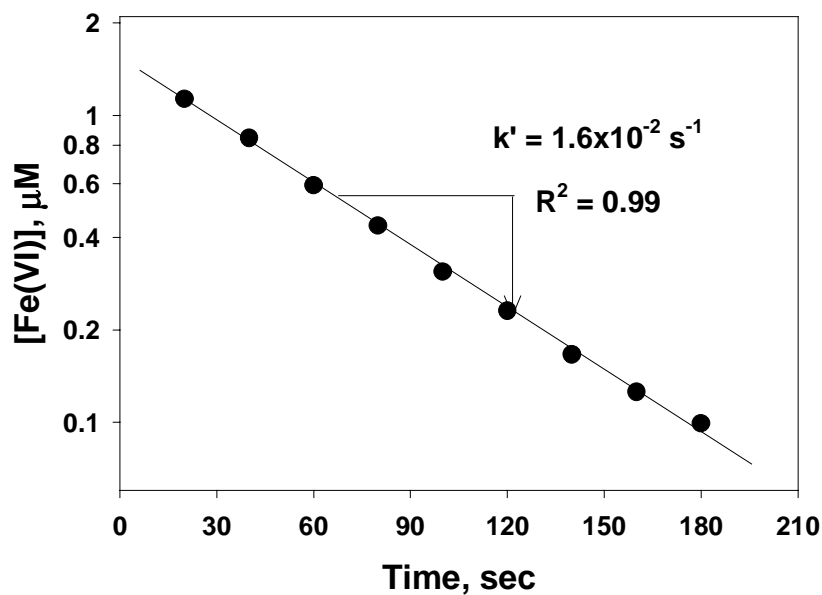


Figure S2. Pseudo-first-order kinetic plot of the consumption of Fe(VI) by excess PhOH (500 μM) at pH 9.0 and 25°C.

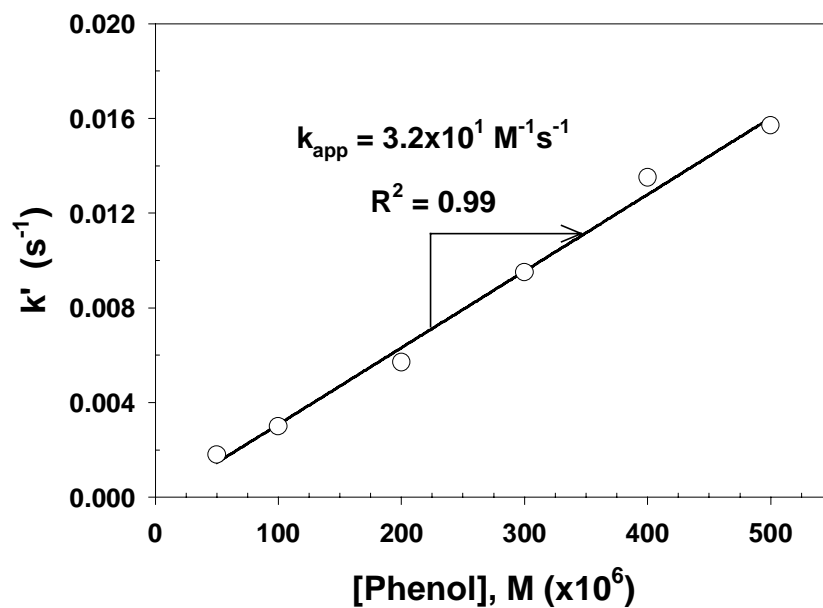


Figure S3. Plot of the pseudo-first-order rate constant for the decrease of Fe(VI) (k') vs initial PhOH concentration at pH 9.0 and 25°C.

Text S4. Determination of second-order rate constant.*1) Phenolic EDCs (EE2, E2, and BPA).*

The apparent second-order rate constants for the selected phenolic EDCs (EE2, E2, and BPA) were determined by monitoring their decrease in the presence of at least a 10 fold excess of Fe(VI). A 250 mL glass bottle with a dispenser system mounted onto the screwtop was used as a reactor. The kinetic runs were begun by adding 5–10 mL of the Fe(VI) stock solution to a solution containing each phenolic EDC (0.25 μM), yielding an initial Fe(VI) concentration of 4–10 μM . The first sample (5 mL) was withdrawn after 20 sec using the dispenser system. Subsequently, 7 more samples were withdrawn at set time intervals ranging from 40 sec to 20 min depending on the apparent oxidation rate of the phenolic EDCs. In addition, it was necessary to measure the rate of Fe(VI) decrease because Fe(VI) is unstable at $\text{pH} < 8$ (1). For this, 3 to 7 samples were collected for the Fe(VI) analysis using the ABTS method. For phenolic EDCs analysis by the HPLC method, the Fe(VI) residuals were immediately quenched by mixing the sample with 0.1 mL ascorbic acid (25 mM). Ascorbic acid reacts rapidly with Fe(VI) (second-order rate constants are above $10^6 \text{ M}^{-1}\text{s}^{-1}$ at pHs 6.8–11.5 ranges) (2) and are found to be a good quenching reagent for Fe(VI). In addition, reduction of oxidation products to parent EDCs by ascorbic acid was not observed within several days after quenching process. Sample analysis by the HPLC methods were conducted within a few hours after sampling. The data was evaluated by plotting the natural logarithm of the phenolic EDCs concentration versus the Fe(VI) exposure, i.e., Fe(VI) concentration integrated over time, as shown in eq 3.

$$\ln([\text{EDC}]/[\text{EDC}]_0) = -k_{\text{app}} \int_0^t [\text{Fe(VI)}] dt \quad (3)$$

where the term $\int_0^t [\text{Fe(VI)}] dt$ represents the Fe(VI) exposure, the time integrated concentration of Fe(VI) and k_{app} (the slope of resulting straight line) represents the apparent second-order rate constant.

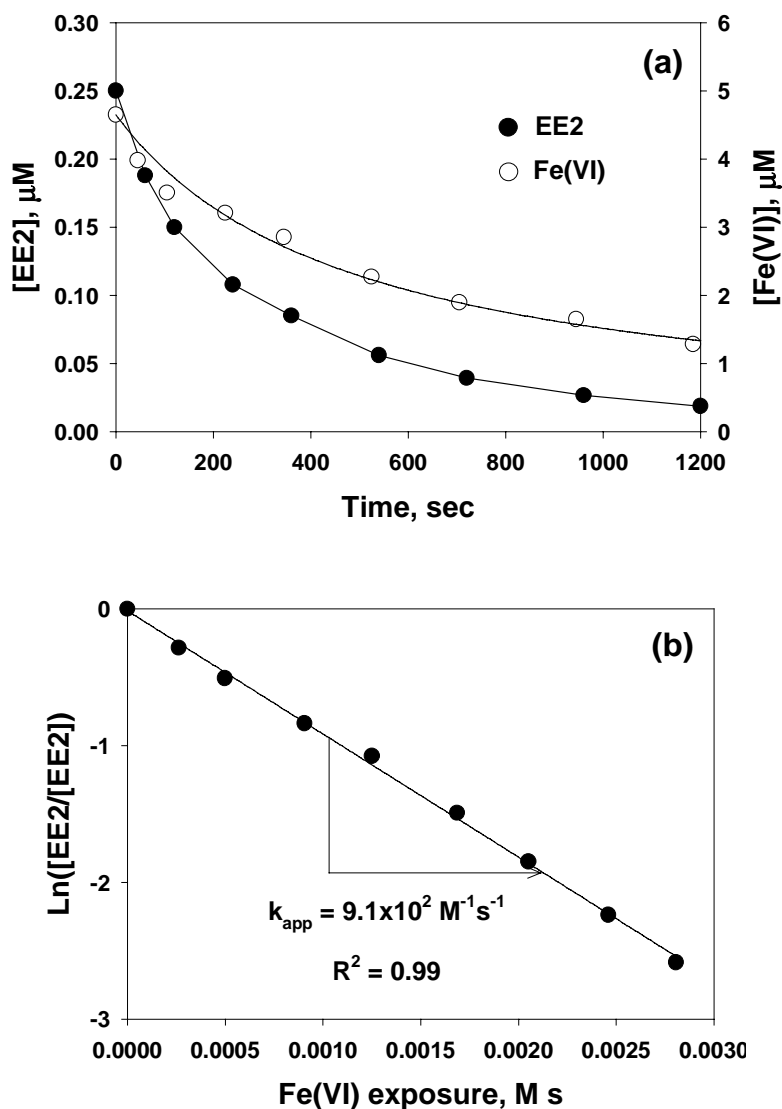


Figure S4. (a) Concentration time profiles of EE2 and Fe(VI). $[\text{EE2}]_0 = 0.25 \mu\text{M}$, $[\text{Fe(VI)}]_0 = 4.7 \mu\text{M}$, pH = 6 (25 mM phosphate buffer), and 25°C , (b) fit of EE2 oxidation by Fe(VI) with second-order reaction kinetics (eq 3).

Figure S4a shows the concentration time profiles of EE2 and Fe(VI) during the oxidation of EE2 (0.25 μM) by excess Fe(VI) (4.7 μM) at pH 6 as a representative data. As expected, Fe(VI) was unstable at pH 6 and about 70% of initial Fe(VI) decayed within 20 min of reaction time. Nonetheless, the Fe(VI) concentration was always in excess to the concentration of EE2 within the studied reaction time ($[\text{EE2}] \ll [\text{Fe(VI)}]$). Figure S4b clearly shows that eq 3 successfully represents the kinetic of EE2 removal by Fe(VI) oxidation ($R^2 > 0.99$). From the slope of the curve in Fig. S4b, the apparent second-order rate constant of EE2 oxidation by Fe(VI) was determined as $k_{\text{app}} = 9.1 \times 10^2 \text{ M}^{-1} \text{ s}^{-1}$ at pH 6 and 25°C.

2) *Substituted Phenols.*

The apparent second-order rate constants for the substituted phenols were determined under the conditions with the substituted phenols in excess. In this case, the decrease in the Fe(VI) concentration was monitored instead of the disappearance of the target compound. The kinetic runs were started by adding 5 mL of the Fe(VI) stock solution to the solution containing each substituted phenol (250 mL), yielding an initial Fe(VI) concentration of 0.5–2.0 μM . The Fe(VI) decrease was monitored using the ABTS method. At these low initial Fe(VI) concentrations (0.5–2.0 μM), the self-decay of Fe(VI) was negligible compared with Fe(VI) decay as a result of its reaction with the substituted phenols. The preliminary experiments showed that the self-decay of Fe(VI) was < 5% within 3 min at an initial Fe(VI) concentration of 1 μM and at pH 6 (data not shown). The data was evaluated by plotting the natural logarithm of the Fe(VI) concentration versus the reaction time. The slope of the resulting straight line represents the pseudo-first-order rate constant. The apparent second-order rate constant was obtained by dividing the pseudo-first-order rate constant by the concentration of the substituted phenols.

Text S5. Lake Zürich Water and Kloten Wastewater.

Lake Zürich water was taken from a depth of 30 m below the surface. Lake Zürich is a deep oligotrophic, seasonally stratified lake with an alpine catchment area. In the conventional activated sludge treatment (CAS) plant in Kloten, the combined sewage of 55,000 population equivalents is treated using a conventional activated sludge system that is equipped with a primary clarifier, nitrification, and denitrification (11 ± 2 days sludge age). The waters were filtered (0.45 μm cellulose nitrate) upon arrival and stored at 4°C until use

Text S6. Critical Evaluation of the Contributions of each Fe(VI) and phenolic EDC species to the Overall Reaction.

The reactions of H_2FeO_4 and FeO_4^{2-} with the phenolic EDCs were neglected in the model calculations due to the following reasons. First, the reactions between H_2FeO_4 and the phenolic EDCs were neglected because the abundance of H_2FeO_4 is rather low within the pH range studied ($\text{pK}_{\text{a,H}_2\text{FeO}_4}$ is 3.5, which is 2.5 pH units lower than the lowest pH value studied). Second, the reactions between FeO_4^{2-} and the phenolic EDCs were neglected based on the following observation. The k_{app} decreased with decreasing HFeO_4^- concentration with increasing pH (See Figure 1 in the main text). This suggests that the overall reactions may be dominated by the reactions involving HFeO_4^- , and that FeO_4^{2-} does not make a significant contribution to the overall reactivity of the phenolic EDCs with Fe(VI). Similar observations, i.e. HFeO_4^- rather than FeO_4^{2-} represents the primary oxidant species in the Fe(VI) reactions, have been reported (1, 3, 4).

Regression analysis of the experimental data with the general model, eq 2 (in the main text), was performed to test above assumption that of the three Fe(VI) species, only HFeO_4^-

contributes significantly to the overall reaction between Fe(VI) and phenolic EDCs. This regression yielded values close to zero for the rate constants k_{ij} corresponding to the reactions omitted from the simplified models (reactions of H_2FeO_4 and FeO_4^{2-}). The exclusion of these values did not significantly affect the model accuracy. This provides additional support for the assumptions made in the model.

Text S7. Ionization Fraction of Fe(VI) and Phenolic Compounds (α_i and β_j).

The values of α_i and β_j can be expressed using the equilibrium constants of Fe(VI) ($K_{a, \text{H}_2\text{FeO}_4} = 3.50$ and $K_{a, \text{HFeO}_4^-} = 7.23$) and the corresponding phenolic compounds as shown below.

1) Ionization fraction of Fe(VI) species

$$\alpha_1 = \frac{[\text{H}_2\text{FeO}_4]}{[\text{Fe(VI)}]_t} = \frac{[\text{H}^+]^2}{T_1}, \alpha_2 = \frac{[\text{HFeO}_4^-]}{[\text{Fe(VI)}]_t} = \frac{[\text{H}^+]K_{a, \text{H}_2\text{FeO}_4}}{T_1}, \alpha_3 = \frac{[\text{FeO}_4^{2-}]}{[\text{Fe(VI)}]_t} = \frac{K_{a, \text{H}_2\text{FeO}_4}K_{a, \text{HFeO}_4^-}}{T_1}, \text{ and}$$

$$T_1 = [\text{H}^+]^2 + [\text{H}^+]K_{a, \text{H}_2\text{FeO}_4} + K_{a, \text{H}_2\text{FeO}_4}K_{a, \text{HFeO}_4^-}$$

2) Ionization fraction of phenolic compounds of monoprotic acids ($K_{a, \text{PhOH}}$): EE2, E2, and all substituted phenols in Table 1)

$$\beta_1 = \frac{[\text{PhOH}]}{[\text{PhOH}]_t} = \frac{[\text{H}^+]}{[\text{H}^+] + K_{a, \text{PhOH}}}, \beta_2 = \frac{[\text{PhO}^-]}{[\text{PhOH}]_t} = \frac{K_{a, \text{PhOH}}}{[\text{H}^+] + K_{a, \text{PhOH}}}$$

3) Ionization fraction of phenolic compounds of diprotic acids ($K_{a, \text{PhOH}}$ and K_{a, PhO^-}): BPA

$$\beta_1 = \frac{[\text{PhOH}]}{[\text{PhOH}]_t} = \frac{[\text{H}^+]^2}{T_2}, \beta_2 = \frac{[\text{PhO}^-]}{[\text{PhOH}]_t} = \frac{[\text{H}^+]K_{a, \text{PhOH}}}{T_2}, \beta_3 = \frac{[\text{PhO}^{2-}]}{[\text{PhOH}]_t} = \frac{K_{a, \text{PhOH}}K_{a, \text{PhO}^-}}{T_2}, \text{ and } T_2 =$$

$$[\text{H}^+]^2 + [\text{H}^+]K_{a, \text{PhOH}} + K_{a, \text{PhOH}}K_{a, \text{PhO}^-}$$

Text S8. Determination of k_{ij} Values by Least Square Regression Analysis.

The specific second-order rate constants, k_{ij} , and the standard errors were determined by a nonlinear least squares regression of the experimental k_{app} data. The regression was performed using the regression function in Microsoft Excel 2002 software. In the regression analysis, eq 6 (main text) was used for EE2 and E2 and eq 7 (main text) was used for BPA.

Text S9. Linear Free Energy Relationships

1) σ Constant.

Hammett-type correlations ($\log k = \log k_0 + \rho\sigma$) were tested for both k_{21} and k_{22} (See Table 1, main text) vs three sets of σ constants, σ^+ , σ , and σ^- (5). The obtained correlation equations are as follows:

$$\log(k_{21}) = 2.24 (\pm 0.05) - 2.27 (\pm 0.17)\sigma^+ \quad r^2 = 0.974, n = 7 \quad (4)$$

$$\log(k_{22}) = 4.33 (\pm 0.08) - 3.60 (\pm 0.18)\sigma^+ \quad r^2 = 0.983, n = 9 \quad (5)$$

$$\log(k_{21}) = 2.41 (\pm 0.14) - 2.99 (\pm 0.51)\sigma \quad r^2 = 0.852, n = 8 \quad (6)$$

$$\log(k_{22}) = 4.66 (\pm 0.16) - 4.30 (\pm 0.38)\sigma \quad r^2 = 0.940, n = 10 \quad (7)$$

$$\log(k_{21}) = 2.46 (\pm 0.10) - 2.97 (\pm 0.34)\sigma^- \quad r^2 = 0.927, n = 8 \quad (8)$$

$$\log(k_{22}) = 4.72 (\pm 0.17) - 3.09 (\pm 0.29)\sigma^- \quad r^2 = 0.935, n = 10 \quad (9)$$

2) pK_a values.

Figure S5 shows good linear relationships for both k_{21} and k_{22} vs pK_a values (See Table 1,

main text). The obtained correlation equations are as shown in eqs 10 and 11.

$$\log(k_{21}) = -11.57 (\pm 2.02) + 1.42 (\pm 0.21) \text{pK}_a \quad r^2 = 0.886, n = 8 \quad (10)$$

$$\log(k_{22}) = -9.62 (\pm 1.45) + 1.45 (\pm 0.16) \text{pK}_a \quad r^2 = 0.916, n = 10 \quad (11)$$

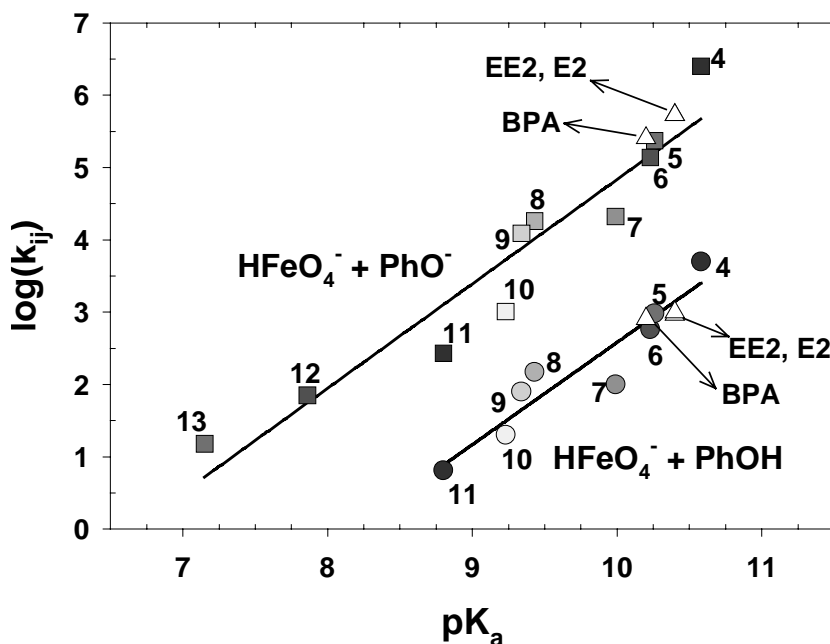


Figure S5. Correlations between the second-order rate constants of the reactions between HFeO_4^- with the undissociated phenols (k_{21}) and the dissociated phenols (k_{22}) vs pK_a values. The numbers of the compounds correspond to those in Table 1 (main text).

If eqs 10 and 11 are used to predict the rate constant of the oxidation of the phenolic compounds by Fe(VI), the following two points should be considered. Firstly, the rate constant for the phenolic compounds with pK_a values are $< \sim 7.9$ can be higher than that predicted using eqs 10 and 11. This is because the reaction between H_2FeO_4 and the dissociated phenol can

contribute significantly to the overall reaction. This phenomenon was observed for 4-cyanophenol and 4-nitrophenol with pK_a values of 7.86 and 7.15, respectively. Secondly, the rate constant predicted using eqs 10 and 11 can differ slightly from the rate constant of phenolic compounds oxidation by Fe(VI) by the stoichiometric factor (η). The value of η can deviate from 1 as a result of fast side reactions of Fe(VI) with the products of the primary reactions. Nevertheless, the values of η for the reaction between the substituted phenols and Fe(VI) are not expected to significantly deviate from 1 based on the reaction scheme proposed for phenol oxidation by Fe(VI) (6, 7). Figure S5 also shows that the plots of k_{21} and k_{22} of EE2, E2, and BPA vs their pK_a are in line with the correlation eqs 10 and 11, respectively. This highlights the success of using eqs 10 and 11 to predict the rate constants of phenolic compounds oxidation by Fe(VI).

3) Estimation of σ^+ , σ , and σ^- constants of EE2, E2, and BPA

The σ^+ , σ , and σ^- constants of EE2, E2, and BPA are not available in the literatures. Since these phenolic EDCs are of great concern in aquatic environments, and in addition they can be readily transformed by several water treatment oxidants, it will be useful to know their σ^+ , σ , and σ^- constants to predict their oxidation rates during water treatment by oxidation. The σ^+ , σ , and σ^- constants of EE2, E2, and BPA are estimated by using eqs 4–9 and the corresponding k_{ij} values (k_{21} and k_{22} in Table 1, main text) determined this study. The values are as follows.

$$\text{EE2: } \sigma^+ = -0.36, \sigma = -0.22, \sigma^- = -0.25$$

$$\text{E2: } \sigma^+ = -0.36, \sigma = -0.22, \sigma^- = -0.25$$

$$\text{BPA: } \sigma^+ = -0.23, \sigma = -0.11, \sigma^- = -0.11$$

Text S10. Oxidation Kinetics of BPA in Natural Water and Wastewater.

Lake Zurich water and Kloten wastewater were spiked with 0.15 μM BPA and treated with Fe(VI) at a dose of 6 and 20 μM , respectively. Figure S6 shows the time-dependent concentrations of EE2 and Fe(VI) during treatment of Lake Zurich water (Fig. S6a) and Kloten wastewater (Fig. S6b), respectively. In addition, Figure S6 shows that the determined rate constants ($k_{\text{Fe(VI)}}$) can be applied to predict BPA removal kinetics in real waters.

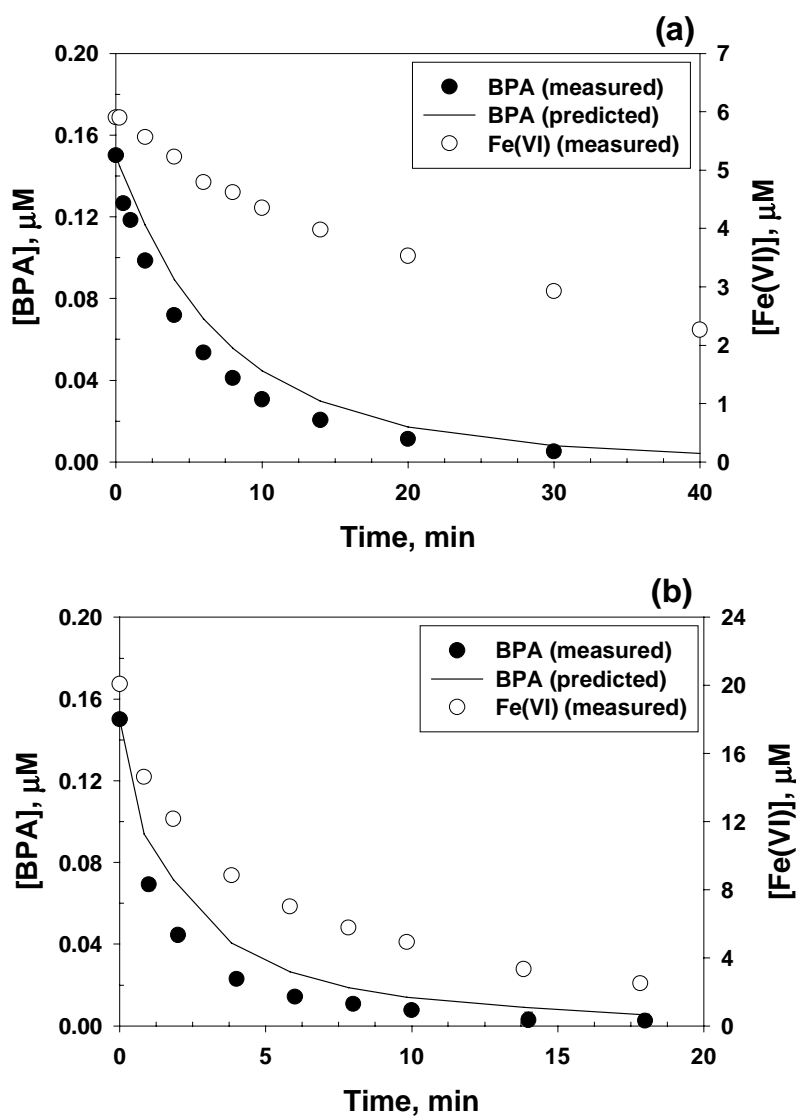


Figure S6. Oxidation kinetics of BPA by Fe(VI) during treatment of (a) lake water and (b)

wastewater. Symbols represent measured data, and solid lines represent model prediction.

Experimental conditions: pH = 8 and T = 25°C.

Literature Cited

- (1) Rush, J. D.; Zhao, Z.; Bielski, B. H. J. Reaction of ferrate(VI)/ferrate(V) with hydrogen peroxide and superoxide anion—a stopped-flow and premix pulse radiolysis study. *Free Rad. Res.* **1996**, *24*, 187–198.
- (2) Cyr, J. E.; Bielski, B. H. J. The reduction of ferrate(VI) to ferrate(V) by ascorbate. *Free. Rad. Biol. Med.* **1991**, 157–160.
- (3) Huang, H.; Sommerfeld, D.; Dunn, B. C.; Lloyd, C. R.; Eyring, E. M. Ferrate(VI) oxidation of aniline. *J. Chem. Soc. Dalton Trans.* **2001**, 1301–1305.
- (4) Sharma, V. K.; Burnett, C. R.; O'Connor, D. B.; Cabelli, D. Iron(VI) and iron(V) oxidation of thiocyanate. *Environ. Sci. Technol.* **2002**, *36*, 4182–4186.
- (5) Hansch C.; Leo, A.; Taft, R. W. A survey of Hammett substituent constants and resonance and field parameters. *Chem. Rev.* **1991**, *91*, 165–195.
- (6) Rush, J. D.; Cyr, J. E.; Zhao, Z.; Bielski, B. H. J. The oxidation of phenol by ferrate(VI) and ferrate(V). A pulse radiolysis and stopped-flow study. *Free Rad. Res.* **1995**, *22*, 349–360.
- (7) Huang, H.; Sommerfeld, D.; Dunn, B. C.; Eyring, E. M.; Lloyd, C. R. Ferrate(VI) oxidation of aqueous phenol: Kinetics and mechanism. *J. Phys. Chem. A.* **2001**, *105*, 3536–3541.